



Published in final edited form as:

Inorg Chem. 2018 October 01; 57(19): 11847–11850. doi:10.1021/acs.inorgchem.8b01130.

Design and Synthesis of Porous Nickel(II) and Cobalt(II) Cages

Eric J. Gosselin, Casey A. Rowland, Krista P. Balto, Glenn P. A. Yap, and Eric D. Bloch*

Department of Chemistry & Biochemistry, University of Delaware, Newark, Delaware 19716, United States

Abstract

Coordination assemblies containing transition-metal cations with coordinatively unsaturated sites remain a challenging target in the synthesis of porous molecules. Herein, we report the design, synthesis, and characterization of three porous hybrid inorganic/organic porous molecular assemblies based on cobalt(II) and nickel(II). Precise tuning of ligand functionalization allows for the isolation of molecular species in addition to two- and three-dimensional metal–organic frameworks. The cobaltous and nickelous cage compounds display excellent thermal stabilities in excess of 473 K and Brunauer–Emmett–Teller surface areas on the order of 200 m²/g. The precise ligand functionalization utilized here to control phases between discrete molecules and higher-dimensional solids can potentially further be tuned to optimize the porosity and solubility in future molecular systems.

Carboxylate-based porous cages are essentially identical with carboxylate-based metal–organic frameworks (MOFs) in terms of their underlying coordination chemistry. However, their synthesis, characterization, and gas adsorption properties are rather divergent, and as a result, the former are relatively underdeveloped. Many of the canonical carboxylate-based MOF structures have been synthesized for a wide variety of transition-metal cations, whereas porous cages that are isostructural across a series of metal cations are rare. As an illustrative example, Cu₃(btc)₂ (HKUST-1) and Cu₂₄(bdc)₂₄ (btc³⁻ = 1,3,5-benzenetricarboxylate; bdc²⁻ = 1,3-benzenedicarboxylate), a three-dimensional MOF and a discrete coordination cage,^{1,2} respectively, were reported within 2 years of each other. The MOF has since been reported for nine transition metals, including every metal in the first row from Cr²⁺ to Zn²⁺.^{3–7} For comparison, in terms of first-row metals, the M₂₄(bdc)₂₄ cuboctahedral structure has only been reported for Cr²⁺ and Cu²⁺.^{8–11} In order to tune the

*Corresponding Author edb@udel.edu.

Notes

The authors declare no competing financial interest.

ASSOCIATED CONTENT

Supporting Information

The Supporting Information is available free of charge on the ACS Publications website at DOI: [10.1021/acs.inorgchem.8b01130](https://doi.org/10.1021/acs.inorgchem.8b01130).

Detailed experimental procedures, structures of materials, and characterization data including powder X-ray diffraction, thermogravimetric analysis, IR spectra, gas adsorption information, and crystallographic information (PDF)

Accession Codes

CCDC 1833892—1833901 and 1833903 contain the supplementary crystallographic data for this paper. These data can be obtained free of charge via www.ccdc.cam.ac.uk/data_request/cif, or by emailing data_request@ccdc.cam.ac.uk, or by contacting The Cambridge Crystallographic Data Centre, 12 Union Road, Cambridge CB2 1EZ, UK; fax: +44 1223 336033.

porosity, stability, and catalytic properties of porous coordination cages, we have great interest in expanding their synthesis to a wider range of first-row transition-metal cations because these have been shown to be amenable to incorporation into paddlewheel building units.

Toward the synthesis of novel porous coordination assemblies, we screened the solvothermal reaction of a library of first-row transition-metal salts with 5-functionalized 1,3-benzenedicarboxylic acid and 9-functionalized carbazoledicarboxylic acid (H_2cdc). Particularly in the case of cobalt(II) and nickel(II), these reactions afforded a variety of crystalline products, including three- and two-dimensional MOFs and discrete coordination cages. The reaction of $NiOAc_2 \cdot 4H_2O$ with H_2bdc in *N,N*-dimethylacetamide (DMA)/methanol (MeOH) at 100 °C for 14 days affords a three-dimensional material, as shown in Figure 1. Interestingly, this material features both nickel(II) paddlewheel units and Ni_3O clusters. The combination of these particular inorganic nodes within MOFs has previously been observed for cobalt and nickel.^{12,13} The structure reported here features large hexagonal channels of approximately 18 Å in diameter in addition to smaller octahedral pores. Given the long reaction time and elevated temperatures required for the reaction coupled with the high Lewis acidity of Ni^{2+} , the nickel cations in the structure feature dimethylamine ligands from decomposed DMA. Solvent exchange with tetrahydrofuran followed by activation under a dynamic vacuum at 150 °C for 48 h resulted in a Brunauer–Emmett–Teller (BET) surface area of 1691 m²/g. Consistent with previously reported nickel paddlewheel-based MOFs,¹⁴ the material displays only moderate adsorption enthalpies for a variety of adsorbates.

Given the close proximity of the 5 positions of bdc^{2-} in this framework structure (Figure S1), functionalized ligands afford lower-dimensional materials. For these, the reaction of $NiOAc_2 \cdot 4H_2O$ or $CoCl_2 \cdot 6H_2O$ with 5-methylbenzenedicarboxylic acid ($H_2Me-bdc$) in a DMA/MeOH mixture at 100 °C affords tetragonal crystals. Single-crystal X-ray diffraction (Figure 2) revealed the materials to be isostructural to the two-dimensional structures previously reported for a number of copper(II) materials.¹⁵ Here bimetallic paddlewheel units are connected via Me-bdc ligands in two dimensions to form layered structures. The square windows of these materials, $Ni(Me-bdc)$ and $Co(Me-bdc)$, are lined with the 5-methyl groups of the bridging ligand, which point to alternating windows in the structure. The other half of the windows feature the metal-bound solvent, either MeOH or dimethylamine from decomposed solvent. Similar nickel(II) paddlewheel-based sheets have been reported for the reaction of nickel with terephthalic acid (or naphthalene dicarboxylic acid) where tetragonal sheets are pillared into a three-dimensional MOF via nickel-coordinated 1,4-diazabicyclo[2.2.2]octane.⁶ Similarly, reaction with 5-ethoxybenzenedicarboxylic acid ($H_2OEt-bdc$) affords materials that are isostructural to $M(Me-bdc)$. These solids, $Co(OEt-bdc)$ and $Ni(OEt-bdc)$, have a similar arrangement of square windows half-lined with ethoxide groups and half-lined with metal-coordinated solvent. Although the two-dimensional structure of these four materials is essentially unchanged, there are significant differences in layer–layer stacking as a result of ligand functionalization with distances of 7.959, 8.281, 8.401, and 8.690, Å for $Co(OEt-bdc)$, $Co(Me-bdc)$, $Ni(Me-bdc)$, and $Ni(OEt-bdc)$, respectively. In contrast to previously reported materials based on Cu^{2+} ,¹⁶ we were unable to tune reaction conditions to produce either hexagonal sheets or discrete

cages. This is likely a result of the relative irreversibility of the M–L bonds for much more highly Lewis acidic Co^{2+} and Ni^{2+} compared to Cu^{2+} .

To avoid isolation of two-dimensional tetragonal materials, bulkier and/or more solubilizing functional groups are desirable. This strategy has been employed for the solvent-free synthesis of porous molecular cages rather than extended materials via mechanochemical techniques.¹⁷ *tert*-Butyl functionalization has been utilized for the preparation of molecular coordination assemblies for chromium,^{11,18} copper,¹⁹ molybdenum,⁸ ruthenium,⁹ and a number of heterobimetallic units.²⁰ Further, for paddlewheel building units with this ligand, higher-dimensional materials have only been reported for copper.²¹ The reaction of nickel(II) or cobalt(II) salts with $\text{H}_2^t\text{Bu-bdc}$, however, afforded the two-dimensional hexagonal material for the former and a strictly amorphous material for the latter. $\text{Ni}^t(\text{Bu-bdc})$ is isostructural to the previously reported copper phases and features a hexagonal tiling of triangular pore windows (Figure 3). This structure is compatible with the presence of bulky ligand groups as a result of the larger interligand distance at the 5 position of isophthalic acid of 10.867(8) Å compared to 7.294(1) Å in the tetragonal phase.

Although ligand functionalization with bulky substituents did not favor the formation of discrete cages, utilizing an isophthalic acid ligand that was previously shown to afford highly soluble porous cages ultimately afforded a nickel paddlewheel-based cage. Here, the reaction of 5-hydroxyisophthalic acid with nickel(II) acetate in a DMA/MeOH mixture for 14 days at 100 °C yielded $\text{Ni}_{24}(\text{OH-bdc})_{24}$ cuboctahedral cages in high yield. Here 12 dinickel paddlewheel units coordinate to 24 5-hydroxyisophthalate ligands to form a polyhedron consisting of 8 triangular faces and 6 square faces. As a result of DMA decomposition over the course of the reaction, the nickel paddlewheels feature axially bound dimethylamine on both the interior and exterior sites. The Ni–Ni distance in the paddlewheel of ~2.65 Å is similar to the Cu–Cu distance of 2.63 Å in $\text{Cu}_{24}(\text{OH-bdc})_{24}$ and significantly longer than the Mo–Mo distance of 2.11 Å in the quadruply bonded paddlewheel units of $\text{Mo}_{24}(\text{OH-bdc})_{24}$.⁸

Zhou and co-workers have previously shown that the size and nuclearity of paddlewheel/dicarboxylic acid-based coordination cages can be judiciously tuned via the utilization of bridging ligands with varying angles between carboxylic acid groups.²² For structures in which the relative irreversibility of metal–ligand bond formation hinders isolation of the crystalline product, this strategy has potential for the synthesis of novel structures. For this, we utilized H_2cdc because the angle between carboxylic acid groups is ~90° and $\text{M}_{12}\text{L}_{12}$ cages containing this ligand have previously been reported for Cu^{2+} , $\text{Ru}^{2+/3+}$, and Mo^{2+} .^{9,23} The reaction of cobalt salts with H_2cdc , however, results in the formation of a two-dimensional hexagonal MOF analogous to $\text{Ni}^t(\text{Bu-bdc})$. This structure similarly features a hexagonal tiling of triangular pores. To the best of our knowledge, this is the first example of a two-dimensional MOF based on this ligand. Similar to 5-functionalization of isophthalic acid, 9-functionalization of H_2cdc allows for the tunability of phases within carbazole-based materials. Here an isopropyl-functionalized ligand was prepared via the alkylation of 9-H-carbazole with isopropyl iodide. The reaction of 9-isopropylcarbazoledicarboxylic acid ($\text{H}_2^i\text{Pr-cdc}$) with $\text{NiOAc}_2 \cdot 4\text{H}_2\text{O}$ (or $\text{CoCl}_2 \cdot 6\text{H}_2\text{O}$) in a DMA/MeOH (DMA/pyridine) mixture at 100 °C (85 °C) for 14 (1) day(s) affords nickel(II) and cobalt(II) cages,

respectively. These octahedral materials, $\text{Ni}_{12}(\text{iPr-cdc})_{12}$ and $\text{Co}_{12}(\text{iPr-cdc})_{12}$ (Figure 4), are comprised of six bimetallic paddlewheel units, with metal–metal distances of 2.66 and 2.71 Å, respectively, and 12 carbazole ligands. As a result of the lower nuclearity of the structure, it displays an internal metal–metal distance of approximately 14 Å compared to ~16.3 Å for the cuboctahedron despite the use of a longer bridging ligand. These cages are analogous to previously reported octahedral cavities within MOFs.^{24–27}

All three cages reported herein retain crystallinity upon solvent exchange, and their thermogravimetric analysis plots indicate moderate porosity. A close investigation of their crystal structures similarly reveals potential porosity because their three-dimensional packing results in potentially accessible channels in the structures upon activation. Accordingly, thorough solvent exchange with amide solvents, followed by replacement with benzene and subsequent freeze-drying,²⁸ affords porous materials with BET (Langmuir) surface areas of 126 (283), 238 (491), and 207 (308) m²/g for $\text{Co}_{12}(\text{iPr-cdc})_{12}$, $\text{Ni}_{12}(\text{iPr-cdc})_{12}$, and $\text{Ni}_{24}(\text{OH-bdc})_{24}$, respectively. To the best of porous carboxylate-based nickel and cobalt cages.²⁹ Although $\text{Ni}_{24}(\text{OH-bdc})_{24}$ loses significant porosity upon activation above 50 °C, likely a result of structural rearrangement because the cages lack three-dimensional interactions, the carbazole-based materials display excellent thermal stability under evacuation, maintaining porosity up to activation temperatures of 200 °C.

In conclusion, the foregoing results demonstrate the importance of ligand functionalization in controlling the phases of cobalt(II) and nickel(II) paddlewheel-based materials. Here, ligand modification allowed for the isolation of a high-surface-area MOF, numerous nonporous two-dimensional MOFs, and three novel porous coordination cages. Although the surface areas displayed by the cages reported here are modest compared to recently reported materials, we hope the approach outlined here will inform the synthesis of additional porous cages and will further allow the tuning of their solubilities, surface areas, and gas adsorption properties. Future work in this direction will focus on expanding the syntheses outlined here to additional transition-metal cations.

Supplementary Material

Refer to Web version on PubMed Central for supplementary material.

ACKNOWLEDGMENTS

We are grateful to the University of Delaware for generous startup funds that made this work possible.

REFERENCES

- (1). Chiu SS-Y; Lo SM-F; Charmant JPH; Orpen AG; Williams IDA Chemically Functionalizable Nanoporous Material $[\text{Cu}_3(\text{TMA})_2(\text{H}_2\text{O})_3]_n$. *Science* 1999, 283, 1149–1150.
- (2). Eddaoudi M; Kim J; Wachter JB; Chae HK; O’Keeffe M; Yaghi OM Porous Metal-Organic Polyhedra: 25 Å Cuboctahedron Constructed from 12 $\text{Cu}_2(\text{CO}_2)_4$ Paddle-Wheel Building Blocks. *J. Am. Chem. Soc* 2001, 123, 4368–4369. [PubMed: 11457217]
- (3). Murray LJ; Dinca M; Yano J; Chavan S; Bordiga S; Brown CM; Long JR Highly-Selective and Reversible O₂ Binding in $\text{Cr}_3(1,3,5\text{-benzetricarboxylate})_2$. *J. Am. Chem. Soc* 2010, 132, 7856–7857. [PubMed: 20481535]

- (4). Zhang Z; Zhang L; Wojtas L; Eddaoudi M; Zaworotko MJ Template-Directed Synthesis of Nets Based upon Octahemioctahedral Cages That Encapsulate Catalytically Active Metalloporphyrins. *J. Am. Chem. Soc* 2012, 134, 928–933. [PubMed: 22208770]
- (5). Xie L; Liu S; Gao C; Cao R; Cao J; Sun C; Su Z Mixed-Valence Iron(II,III) Trimesates with Open Frameworks Modulated by Solvents. *Inorg. Chem* 2007, 46, 7782. [PubMed: 17696421]
- (6). Maniam P; Stock N Investigation of Porous Ni-Based Metal-Organic Frameworks Containing Paddle-Wheel Type Inorganic Building Units Via High-Throughput Methods. *Inorg. Chem* 2011, 50, 5085. [PubMed: 21539354]
- (7). Feldblyum JI; Liu M; Gidley DW; Matzger AJ Reconciling the Discrepancies between Crystallographic Porosity and Guest Access As Exemplified by Zn-HKUST-1. *J. Am. Chem. Soc* 2011, 133, 18257–18263. [PubMed: 22011056]
- (8). Ke Y; Collins DJ; Zhou H-C Synthesis and Structure of Cuboctahedral and Anticuboctahedral Cages Containing 12 Quadruply Bonded Dimolybdenum Units. *Inorg. Chem* 2005, 44, 4154–4156. [PubMed: 15934744]
- (9). Young MD; Zhang Q; Zhou H-C Metal-organic polyhedral constructed from dinuclear ruthenium paddlewheels. *Inorg. Chim. Acta* 2015, 424, 216–220.
- (10). Furukawa S; Horike N; Kondo M; Hijikata Y; Carne-Sanchez A; Larpent P; Louvain N; Diring S; Sato H; Matsuda R; Kawano R; Kitagawa S Rhodium-Organic Cuboctahedra as Porous Solids with Strong Binding Sites. *Inorg. Chem* 2016, 55, 10843–10846. [PubMed: 27748586]
- (11). Park J; Perry Z; Chen Y-P; Bae J; Zhou H-C Chromium(II) Metal-Organic Polyhedra as Highly Porous Materials. *ACS Appl. Mater. Interfaces* 2017, 9, 28064–28068. [PubMed: 28741931]
- (12). Shen J-Q; Liao P-Q; Zhou D-D; He C-T; Wu J-X; Zhang W-X; Zhang J-P; Chen X-M Modular and Stepwise Synthesis of a Hybrid Metal-Organic Framework for Efficient Electrocatalytic Oxygen Evolution. *J. Am. Chem. Soc* 2017, 139, 1778–1781. [PubMed: 28112923]
- (13). Wei Y-S; Shen J-Q; Liao P-Q; Xue W; Zhang J-P; Chen X-M Synthesis and stabilization of a hypothetical porous framework based on a classic flexible metal carboxylate cluster. *Dalton Trans* 2016, 45, 4269–4273. [PubMed: 26575992]
- (14). Wade CR; Dinca M Investigation of the synthesis, activation, and isosteric heats of CO₂ adsorption of the isostructural series of metal-organic frameworks M₃(BTC)₂ (M = Cr, Fe, Ni, Cu, Mo, Ru). *Dalton Trans* 2012, 41, 7931–7938. [PubMed: 22539456]
- (15). Abourahma H; Bodwell GJ; Lu J; Moulton B; Pottier IR; Walsh RB; Zaworotko MJ Coordination Polymers from Calixarene-Like [Cu₂(Dicarboxylate)₂]₄ Building Blocks: Structural Diversity via Atropisomerism. *Cryst. Growth Des* 2003, 3, 513–519.
- (16). Barreda O; Bannwart G; Yap GPA; Bloch ED Ligand-Based Phase Control in Porous Molecular Assemblies. *ACS Appl. Mater. Interfaces* 2018, 10, 11420–11424. [PubMed: 29578673]
- (17). Barreda O; Taggart GA; Rowland CA; Yap GPA; Bloch ED Mechanochemical Synthesis of Porous Molecular Assemblies. *Chem. Mater* 2018, just accepted.
- (18). Lorzing GR; Trump BA; Brown CM; Bloch ED Selective Gas Adsorption in Highly Porous Chromium(II)-Based Metal-Organic Polyhedra. *Chem. Mater* 2017, 29, 8583–8587.
- (19). Li JR; Zhou H-C Bridging-ligand-substitution strategy for the preparation of metal-organic polyhedra. *Nat. Chem* 2010, 2, 893–898. [PubMed: 20861907]
- (20). Teo JM; Coghlan CJ; Evans JD; Tsivion E; Head-Gordon M; Sumbly CJ; Doonan CJ Hetero-bimetallic metal-organic polyhedra. *Chem. Commun* 2016, 52, 276–279.
- (21). Wang X-F; Li L; Kong Y-M; Liu Y Spontaneously resolved 2D chiral kagome Cu(II) coordination polymer. *Inorg. Chem. Commun* 2012, 21, 72–75.
- (22). Li J-R; Yakovenko AA; Lu W; Timmons DJ; Zhuang W; Yuan D; Zhou H-C Ligand Bridging-Angle-Driven Assembly of Molecular Architectures Based on Quadruply Bonded Mo-Mo Dimers. *J. Am. Chem. Soc* 2010, 132, 17599–17610. [PubMed: 21082847]
- (23). Li J-R; Timmons DJ; Zhou H-C Interconversion between Molecular Polyhedra and Metal-Organic Frameworks. *J. Am. Chem. Soc* 2009, 131, 6368–6369. [PubMed: 19374418]
- (24). Tian D; Chen Q; Li Y; Zhang Y-H; Chang Z; Bu X-H A Mixed Molecular Building Block Strategy for the Design of Nested Polyhedron Metal-Organic Frameworks. *Angew. Chem., Int. Ed* 2014, 53, 837–841.

- (25). Gao Q; Xu J; Cao D; Chang Z; Bu X-H A Rigid Nested Metal-Organic Framework Featuring a Thermoresponsive Gating Effect Dominated by Conterions. *Angew. Chem., Int. Ed* 2016, 55, 15027– 15030.
- (26). Lu W; Yuan D; Makal TA; Wei Z; Li J-R; Zhou H-C *Dalton Trans* 2013, 42, 1708–1714. [PubMed: 23160711]
- (27). Stoeck U; Krause S; Bon V; Senkovska I; Kaskel S A highly porous metal-organic framework constructed from a cuoboctahedral super-molecular building block, with exceptionally high methane uptake. *Chem. Commun* 2012, 48, 10841–10843.
- (28). Ma L; Jin A; Xie Z; Lin W Freeze Drying Significantly Increases Permanent Porosity and Hydrogen Uptake in 4,4-Connected Metal-Organic Frameworks. *Angew. Chem., Int. Ed* 2009, 48, 9905– 9908.
- (29). Fang Y; Xiao Z; Li J; Lollar C; Liu L; Lian X; Yuan S; Banerjee S; Zhang P; Zhou H-C Formation of a Highly Reactive Cobalt Nanocluster Crystal within a Highly Negatively Charged Porous Coordination Cage. *Angew. Chem., Int. Ed* 2018, 57, 5283–5287.

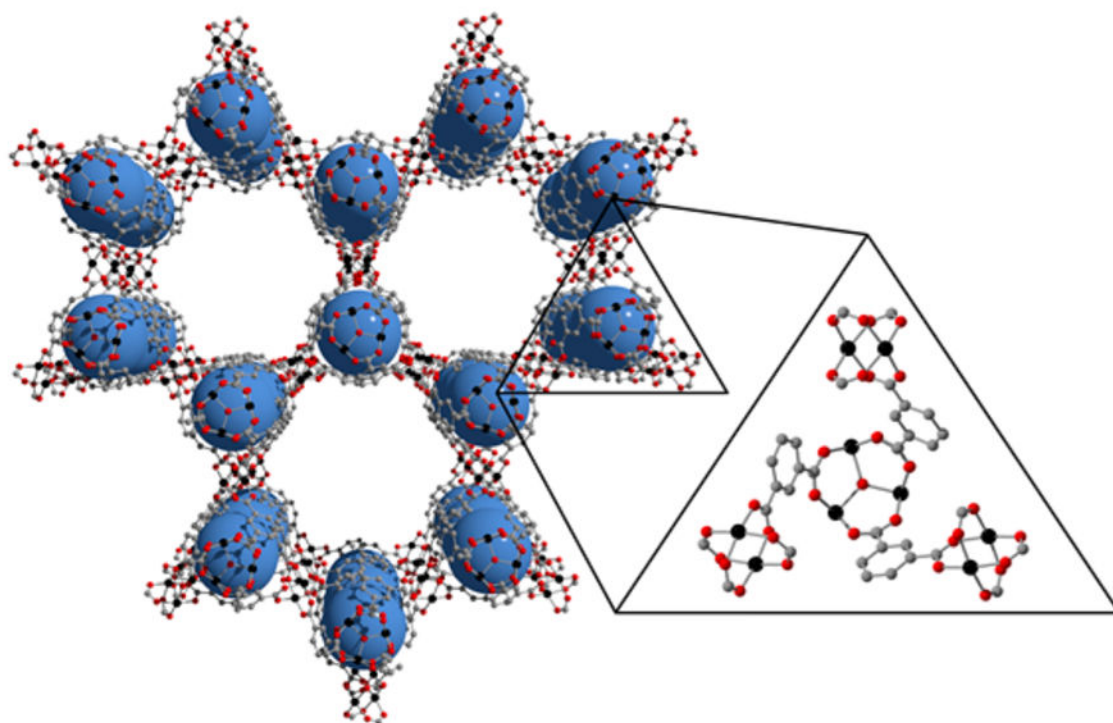
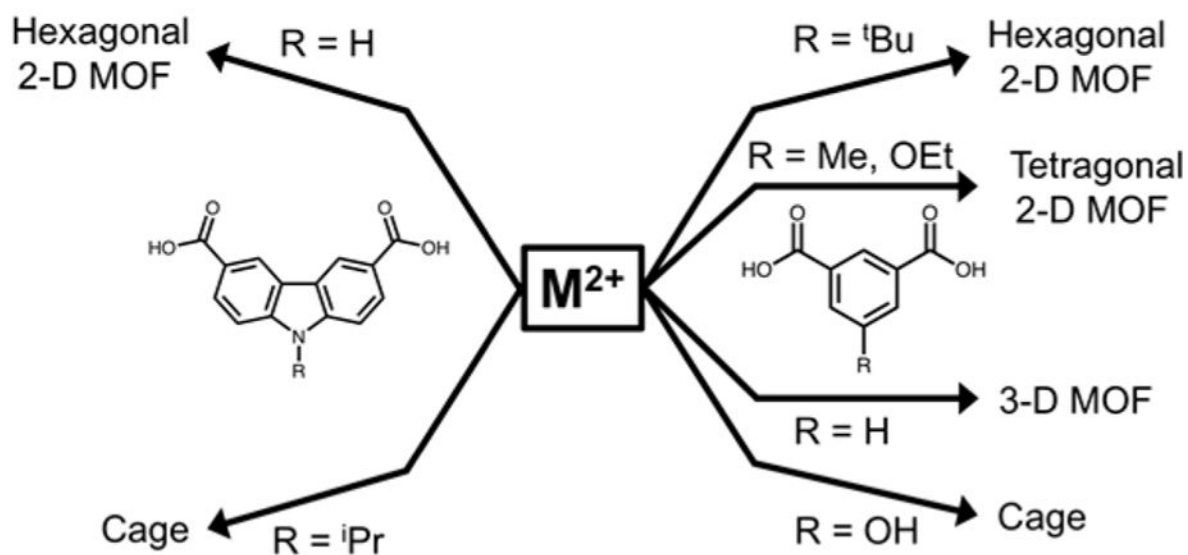


Figure 1.

(Top) Effect of ligand functionalization on the resulting phase of nickel- and cobalt-based materials. (Bottom) Portion of the structure of the nickel framework as determined by single-crystal X-ray diffraction. Black, gray, and red spheres represent nickel, carbon, and oxygen, respectively. Hydrogen atoms and nickel-bound solvent molecules have been omitted. The blue sphere illustrates the smaller of two pores in the structure.

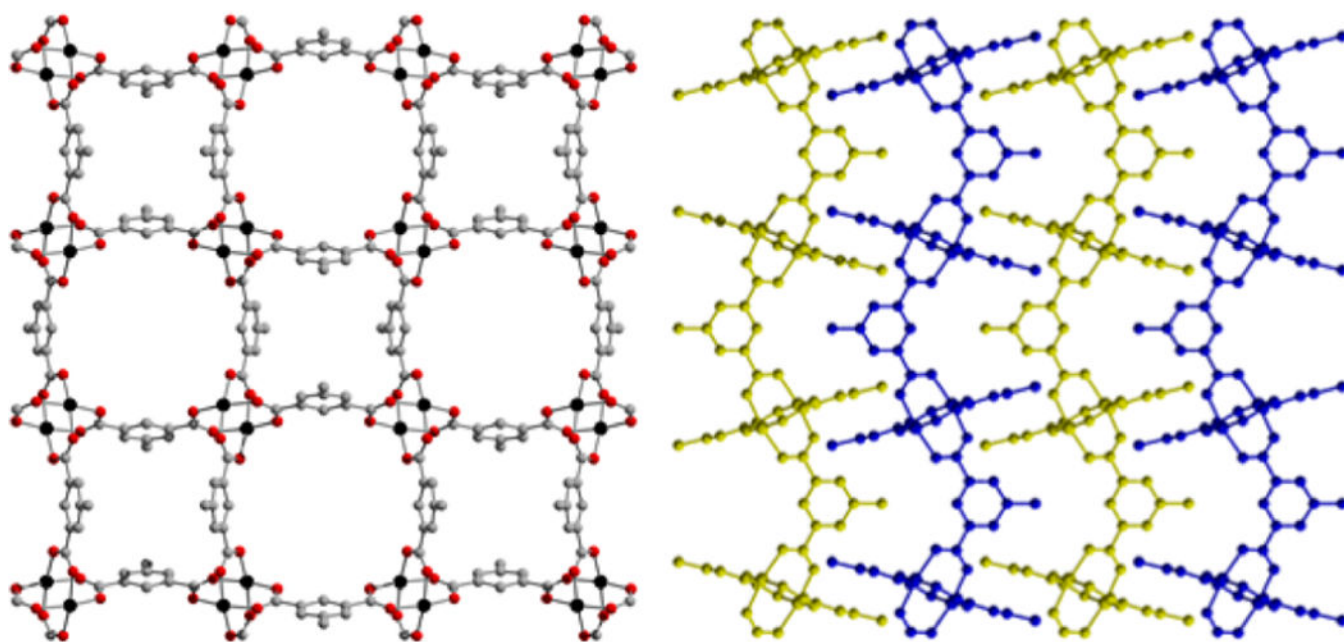


Figure 2. Portion of the structure of the two-dimensional Ni(Me-bdc) framework viewed down the *c* (left) and *b* (right) axes as determined by single-crystal X-ray diffraction. Black, gray, and red spheres represent nickel, carbon, and oxygen, respectively. The two-dimensional sheets stack with a layer–layer distance of 8.299(2) Å.

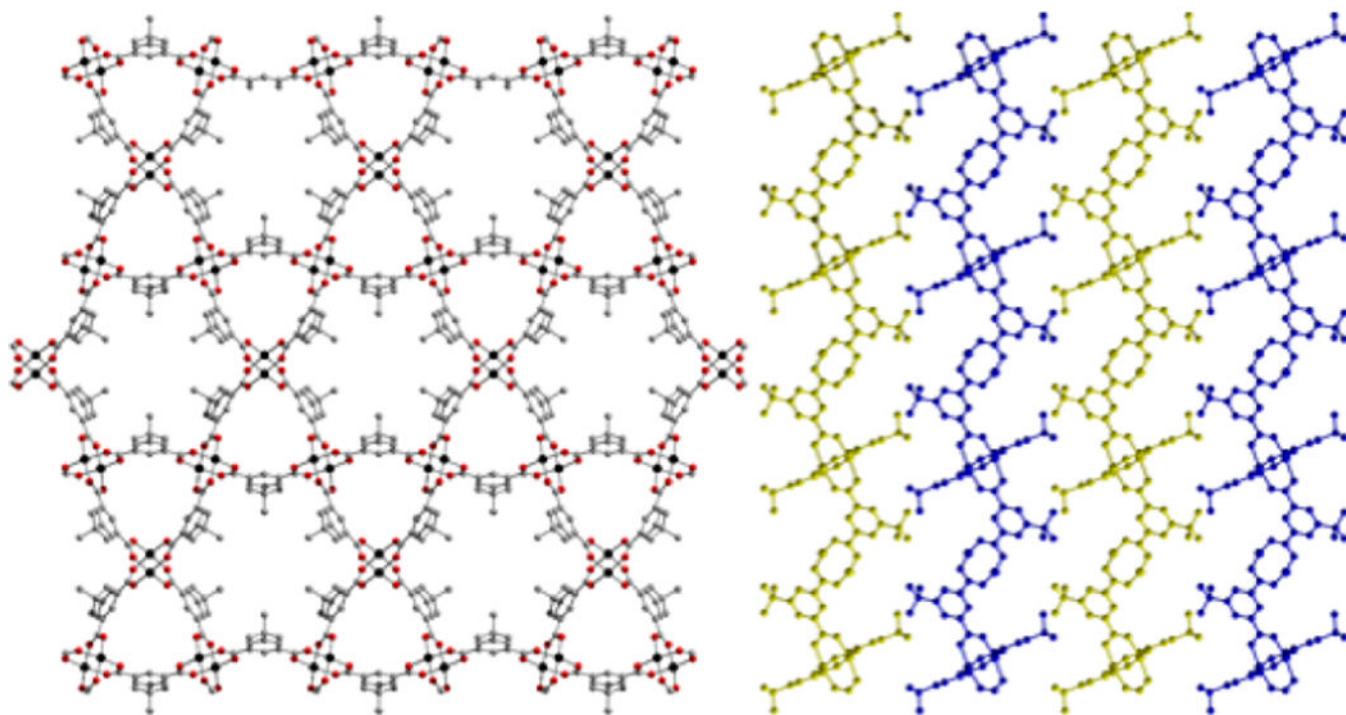


Figure 3.

Portion of the structure of the two-dimensional Ni(⁴Bu-bdc) hexagonal framework viewed down the *c* (left) and *b* (right) axes as determined by single-crystal X-ray diffraction. Black, gray, and red spheres represent nickel, carbon, and oxygen, respectively. The two-dimensional sheets stack with a layer–layer distance of 11.878(1) Å.

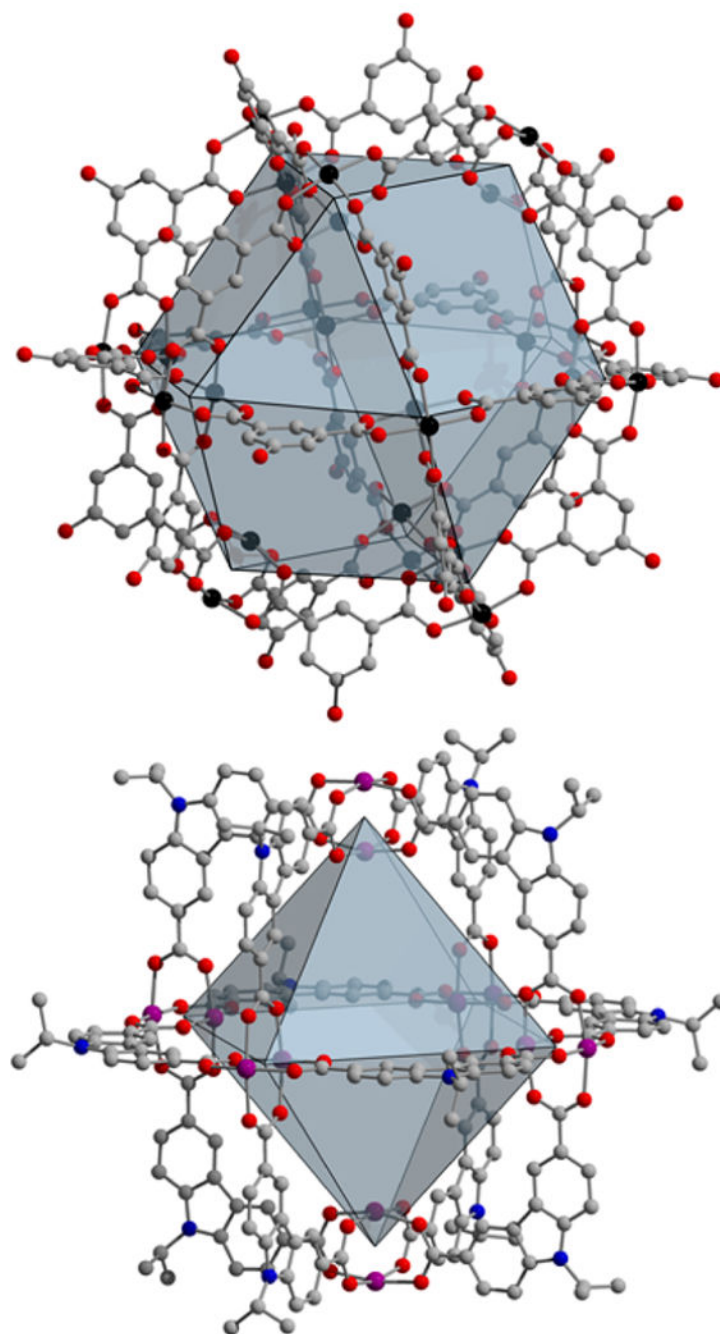


Figure 4. Structures of $\text{Ni}_{24}(\text{OH-bdc})_{24}$ (top) and $\text{Co}_{12}(\text{iPr-cdc})_{12}$ (bottom). Black, purple, gray, red, and blue spheres represent nickel, cobalt, carbon, oxygen, and nitrogen, respectively. The large dark-blue polyhedra represent the potential porosity intrinsic to specific cages.